Communications in Physics, Vol. 35, No. 4 (2025), pp. 379-388
DOI: https://doi.org/10.15625/0868-3166/22871

Influence of magnetic field and temperature on negative refractive index in a degenerate three-level atomic system

Nguyen Huy Bang[1], **Luong Thi Yen Nga**[1], **Nguyen Van Ai**[2], **Nguyen Van Phu**[1], **Phan Duc Thuan**[3] **and Le Van Doai**[1,†]

[1]*Vinh University, 182 Le Duan Street, Nghe An Province, Vietnam*

[2]*Ha Tinh University, 447, 26/3 Street, Ha Tinh Province, Vietnam*

[3]*Hong Lam Technology and Economics College, 382 Le Viet Thuat Street, Nghe An Province, Vietnam*

E-mail: †doailv@vinhuni.edu.vn

Received 13 May 2025
Accepted for publication 18 August 2025
Published 9 December 2025

Abstract. *This work investigates the manipulation of the negative refractive index in a degenerate three-level Λ-type atomic system in the presence of an external magnetic field and Doppler broadening. The results show that the bandwidth of the negative refractive index can be significantly broadened by increasing the coupling laser intensity; for example, when* Ω_c *increases from* 30γ *to* 60γ*, the bandwidth expands from* $[0.5\gamma, 1.5\gamma]$ *to* $[1.2\gamma, 4\gamma]$*. The spectral position can be flexibly tuned by adjusting the magnetic field, shifting toward lower (higher) frequencies for* $B = -1\gamma_c$ *(*$B = 2\gamma_c$*). Temperature has a pronounced effect on both the range and amplitude; increasing the temperature from* 200 K *to* 400 K *narrows the range from* $[-1.6\gamma_c, -0.2\gamma_c]$ *to* $[-1.1\gamma_c, -0.5\gamma_c]$*. These findings may facilitate experimental realization and potential practical applications of EIT-based negative-index materials.*

Keywords: effects of atomic coherence; chiral media; refractive index.

Classification numbers: 42.50.Gy; 81.05.Xj; 78.20.Ci.

1. Introduction

The refractive index is a key parameter that characterizes the optical properties of a medium. Based on Maxwell's equations, the refractive index (n) is determined by the relationship between the relative permittivity (ε_r) and relative permeability (μ_r) as [1]. In conventional optical materials, both $\varepsilon_r > 0$ and $\mu_r > 0$, resulting in a positive refractive index. In this case, the wave vector **k**, the electric field **E** and the magnetic field **H** of a light field form a right-handed system. However, in 1968, Veselago [2] theoretically proposed the existence of a medium in which both the permittivity and permeability are negative ($\varepsilon_r < 0$ and $\mu_r < 0$). In such a medium, the refractive

index becomes negative, and the vectors **k**, **E** and **H** of the light field form a left-handed system. This material is known as left-handed material (LHM) or negative index material (NIM), and their existence was experimentally confirmed a few decades later [3, 4]. Negative index materials have become a major focus of research due to their unique electromagnetic properties and promising applications across a range of fields, including reversed Doppler shift and Cherenkov radiation [2], subwavelength focusing [5], negative Goos-Hänchen shift [6], the realization of a perfect lens [7], and the suppression of spontaneous emission [8], among others.

Various approaches have been developed to realize NIM, such as artificially engineered metamaterials [9], photonic crystal structures [10], transmission line analogs [11], and chiral media [12]. However, most of these implementations operate at high frequencies and are often accompanied by significant absorption losses. Consequently, the development of low-loss negative index materials that function in the optical frequency range remains a subject of intense research interest. In recent years, the realization of negative refractive index in atomic gas media has been achieved through electromagnetically induced transparency (EIT) [13]. In principle, a negative refractive index can be achieved in EIT-based media because, under EIT condition, the magnetic dipole moment can be comparable in magnitude to the electric dipole moment, allowing both the relative permittivity and permeability to be negative simultaneously. Using the EIT effect, Oktel *et al.* [14] and Shen *et al.* [15] were among the first to propose a scheme for generating a negative refractive index in a three-level Λ-type atomic system. Subsequently, Krowne *et al.* [16] demonstrated the realization of a negative index using dressed-state transitions involving mixed parity states. Zhao *et al.* have produced negative refractive index without absorption [17]. This EIT approach offers several notable advantages: first, it enables the realization of a negative refractive index in the optical frequency range without significant absorption; second, both the magnitude and the spectral range of the negative refractive index can be effectively controlled using external fields.

Previous studies on negative refraction in EIT-based materials have often neglected the Doppler effect, making their results applicable primarily to ultra-cold atomic systems, such as those confined in a magneto-optical trap (MOT). However, to extend the applicability of EIT materials to practical conditions across a range of temperatures, several studies have incorporated Doppler broadening into the analysis of EIT [18], as well as its applications—including group velocity control [19], pulse propagation [20], and Kerr nonlinearity [21]. These studies have shown that Doppler broadening significantly affects the EIT phenomenon and related quantities at room temperature.

In recent years, we have also carried out several studies on the negative refractive index based on EIT under various conditions [22–24]. For instance, in Ref. [22], we achieved the negative refractive index at room temperature by including the Doppler effect; in Ref. [23], the negative refractive index was controlled by an external magnetic field in the absence of Doppler broadening; and in Ref. [24], the negative refractive index was realized in two distinct frequency regions. Also, numerous studies on negative refractive index based on EIT have also attracted considerable attention in recent years [25–27].

In this paper, we study the negative refractive index in a degenerate three-level lambda-type atomic system under realistic conditions, including the presence of an external magnetic field and Doppler broadening. The influences of the coupling laser intensity, external magnetic field, and temperature on the negative refractive index are investigated.

2. Theoretical model

Figure 1 illustrates the configuration of a degenerate three-level Λ-type atomic system subjected to an external magnetic field and interacting with both probe and coupling fields. The magnetic field B is assumed to be aligned with the direction of the light beams. When the magnetic field is applied, the ground-state sublevels $|1\rangle$, $|2\rangle$ and $|3\rangle$ become split due to the Zeeman effect. The Zeeman shifts of these levels are determined as $\Delta_B = g_F \mu_B m_F B$, with μ_B the Bohr magneton, g_F the Landé factor and m_F the magnetic quantum number. We assume that the levels $|1\rangle$ and $|2\rangle$ have opposite parity, allowing an electric dipole transition $|1\rangle \leftrightarrow |2\rangle$ where **d** is the electric dipole operator. In contrast, levels $|1\rangle$ and $|3\rangle$ have the same parity, enabling a magnetic dipole transition $|1\rangle \leftrightarrow |3\rangle$ where **m** is the magnetic dipole operator. Hence, the electric and magnetic components of the probe field with the same frequency ω_p can drive the transitions $|1\rangle \leftrightarrow |2\rangle$ and $|1\rangle \leftrightarrow |3\rangle$, simultaneously. The strong coupling field with the frequency ω_c drives the transition $|3\rangle \leftrightarrow |2\rangle$. In this setup, the probe and coupling fields are chosen to be left- (σ^-) and right- (σ^+) circularly polarized light, respectively. Accordingly, the three atomic states are identified as

$$|1\rangle = |S_{1/2}, F = 1, m_F = +1\rangle, \quad |2\rangle = |P_{3/2}, F' = 2, m_F = 0\rangle, \quad |3\rangle = |S_{1/2}, F = 1, m_F = -1\rangle.$$

The spontaneous decay rates from the $|2\rangle$ level to the $|1\rangle$ and $|3\rangle$ levels are denoted by γ_{21} and γ_{23}, respectively, while the relaxation rate between the ground states $|1\rangle$ and $|3\rangle$ is given by γ_{31}.

The time-evolution equation of the system is governed by the Liouville equation:

$$\dot{\rho} = -\frac{i}{\hbar}[H, \rho] + \Lambda\rho, \tag{1}$$

where $\Lambda\rho$ represents the relaxation processes.

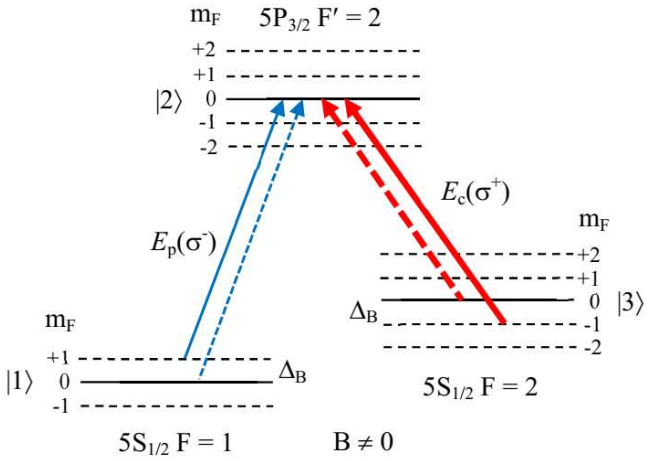

Fig. 1. Schematic of a degenerate three-level Λ-type configuration in a ^{87}Rb atom under an external magnetic field and interacting with two laser fields. The dashed arrows indicate the excitation pathways when the magnetic field is absent ($B = 0$).

In the interaction picture, the total Hamiltonian of the system can be written as [23]

$$H = -\hbar\Delta_p |2\rangle\langle 2| - \hbar(\Delta_p - \Delta_c - 2\Delta_B)|3\rangle\langle 3| - \hbar\left(\Omega_p |2\rangle\langle 1| + \Omega_c |2\rangle\langle 3| + \text{H.c.}\right). \tag{2}$$

From Eqs. (1) and (2), the density matrix equations of the system may be derived under the dipole and rotating wave approximations as:

$$\dot{\rho}_{21} = -\left(i\Delta_p + \frac{\gamma_{21}}{2}\right)\rho_{21} + i\Omega_p(\rho_{11} - \rho_{22}) + i\Omega_c\rho_{23}, \tag{3a}$$

$$\dot{\rho}_{23} = -\left[i(\Delta_p - \Delta_c - 2\Delta_B) + \frac{\gamma_{23}}{2}\right]\rho_{23} + i\Omega_c(\rho_{33} - \rho_{22}) + i\Omega_p\rho_{21}, \tag{3b}$$

$$\dot{\rho}_{31} = -\left[i(\Delta_p - \Delta_c - 2\Delta_B) + \frac{\gamma_{31}}{2}\right]\rho_{31} + i\Omega_c\rho_{21} - i\Omega_p\rho_{32}. \tag{3c}$$

We assume that the atom initially populates the state $|1\rangle$, i.e. $\rho_{11} = 1$, and $\rho_{22} = \rho_{33} = 0$. Solving Eqs. (3a)–(3c) in the steady state ($\dot{\rho} = 0$), we obtain [23]:

$$\rho_{21} = \frac{i\Omega_p(\Delta_p - \Delta_c - 2\Delta_B + i\gamma_{23}/2)}{(\Delta_p + i\gamma_{21}/2)(\Delta_p - \Delta_c - 2\Delta_B + i\gamma_{23}/2) - \Omega_c^2}, \tag{4}$$

$$\rho_{31} = \frac{i\Omega_p\Omega_c}{(\Delta_p + i\gamma_{21}/2)(\Delta_p - \Delta_c - 2\Delta_B + i\gamma_{23}/2) - \Omega_c^2}. \tag{5}$$

The electric susceptibility and magnetic susceptibility of the medium are given by [14]:

$$\chi_e = \frac{Nd_{21}\rho_{21}}{\varepsilon_0 E_p}, \tag{6}$$

$$\chi_m = \frac{Nm_{31}\rho_{31}}{\mu_0 H_p}. \tag{7}$$

The relative permittivity and permeability follow as:

$$\varepsilon_r = 1 + \chi_e, \tag{8}$$

$$\mu_r = 1 + \chi_m. \tag{9}$$

Substituting Eqs. (4) and (5) into Eqs. (6) and (7), one obtains [23]:

$$\chi_e = \frac{A(\Delta_p - \Delta_c - 2\Delta_B + i\gamma_{23}/2)}{(\Delta_p + i\gamma_{21}/2)(\Delta_p - \Delta_c - 2\Delta_B + i\gamma_{23}/2) - \Omega_c^2}, \tag{10}$$

$$\chi_m = \frac{B\Omega_c}{(\Delta_p + i\gamma_{21}/2)(\Delta_p - \Delta_c - 2\Delta_B + i\gamma_{23}/2) - \Omega_c^2}, \tag{11}$$

where $A = Nd_{21}^2/(\varepsilon_0\hbar)$ and $B = Nm_{31}^2/(\mu_0\hbar c^2)$.

Squaring both sides of Eq. (11) yields:

$$\chi_m^2 = \frac{B^2\Omega_c^2}{[(\Delta_p + i\gamma_{21}/2)(\Delta_p - \Delta_c - 2\Delta_B + i\gamma_{23}/2) - \Omega_c^2]^2}. \tag{12}$$

Let

$$Z = (\Delta_p + i\gamma_{21}/2)(\Delta_p - \Delta_c - 2\Delta_B + i\gamma_{23}/2) - \Omega_c^2. \tag{13}$$

Then Eq. (12) becomes:

$$\chi_m^2 = \frac{B^2\Omega_c^2}{Z^2}. \tag{14}$$

Solving for Z gives:

$$Z = \pm B\Omega_c\chi_m^{-1}. \tag{15}$$

To include Doppler broadening, we consider atoms with velocity v along the propagation direction of the lasers. The Doppler-shifted detunings are:

$$\Delta_p \to \Delta_p - kv, \qquad \Delta_c \to \Delta_c - kv,$$

where k is the wave number.

The Maxwell-Boltzmann velocity distribution is:

$$f(v) = N_0 \sqrt{\frac{m}{2\pi k_B T}} \exp\left(-\frac{mv^2}{2k_B T}\right). \tag{16}$$

The Doppler-averaged electric susceptibility is:

$$\chi_e(D) = \int_{-\infty}^{+\infty} \chi_e(v) f(v)\, dv, \tag{17}$$

which evaluates to:

$$\chi_e(D) = A \frac{\sqrt{\pi}}{2ku} e^{z^2} \left[1 - \mathrm{erf}(z)\right], \tag{18}$$

where

$$u = \sqrt{\frac{2k_B T}{m}}, \qquad z = \frac{i(\Delta_p - \Delta_c - 2\Delta_B) + \gamma_{23}/2}{ku}. \tag{19}$$

Similarly, the magnetic susceptibility with Doppler broadening is:

$$\chi_m(D) = B\Omega_c \frac{\sqrt{\pi}}{2ku} e^{z^2} \left[1 - \mathrm{erf}(z)\right], \tag{20}$$

where

$$z = \frac{i(\Delta_p - \Delta_c - 2\Delta_B) + \gamma_{21}/2}{ku}. \tag{21}$$

The Doppler-broadened relative permittivity and permeability are:

$$\varepsilon_r(D) = 1 + \chi_e(D), \tag{22}$$

$$\mu_r(D) = 1 + \chi_m(D). \tag{23}$$

Finally, the refractive index is computed as [14]:

$$n = \sqrt{\varepsilon_r(D)\, \mu_r(D)}. \tag{24}$$

3. Results and discussion

In this study, we used ^{87}Rb atoms to investigate how the negative refractive index depends on optical and magnetic fields in the presence of Doppler broadening. The atomic parameters used are taken from Refs. [14, 23]: atomic density $N = 10^{23}\,\mathrm{atoms/m^3}$, $\gamma_{21} = \gamma_{23} = 5.3\,\mathrm{MHz}$, $g_F = -1/2$ and $\mu_B = 9.27401 \times 10^{-24}\,\mathrm{J/T}$. In the numerical simulations that follow, all frequency-related quantities are normalized by γ, which is on the order of MHz for alkali atoms. Under this normalization, when the Zeeman shift Δ_B is expressed in units of γ, the corresponding magnetic field strength B is given in terms of a combined constant γ_c, which has units of Tesla. For instance, a Zeeman shift of $\Delta_B = 1\gamma$ corresponds to a magnetic field strength of $B = 1\gamma_c$.

First, we consider the case where the external magnetic field is turned off ($B = 0$ or $\Delta_B = 0$) and investigate how the negative refractive index depends on the coupling laser intensity. In Fig. 2, we set the coupling laser detuning $\Delta_c = 0$ and plot the real parts of the relative permittivity (solid

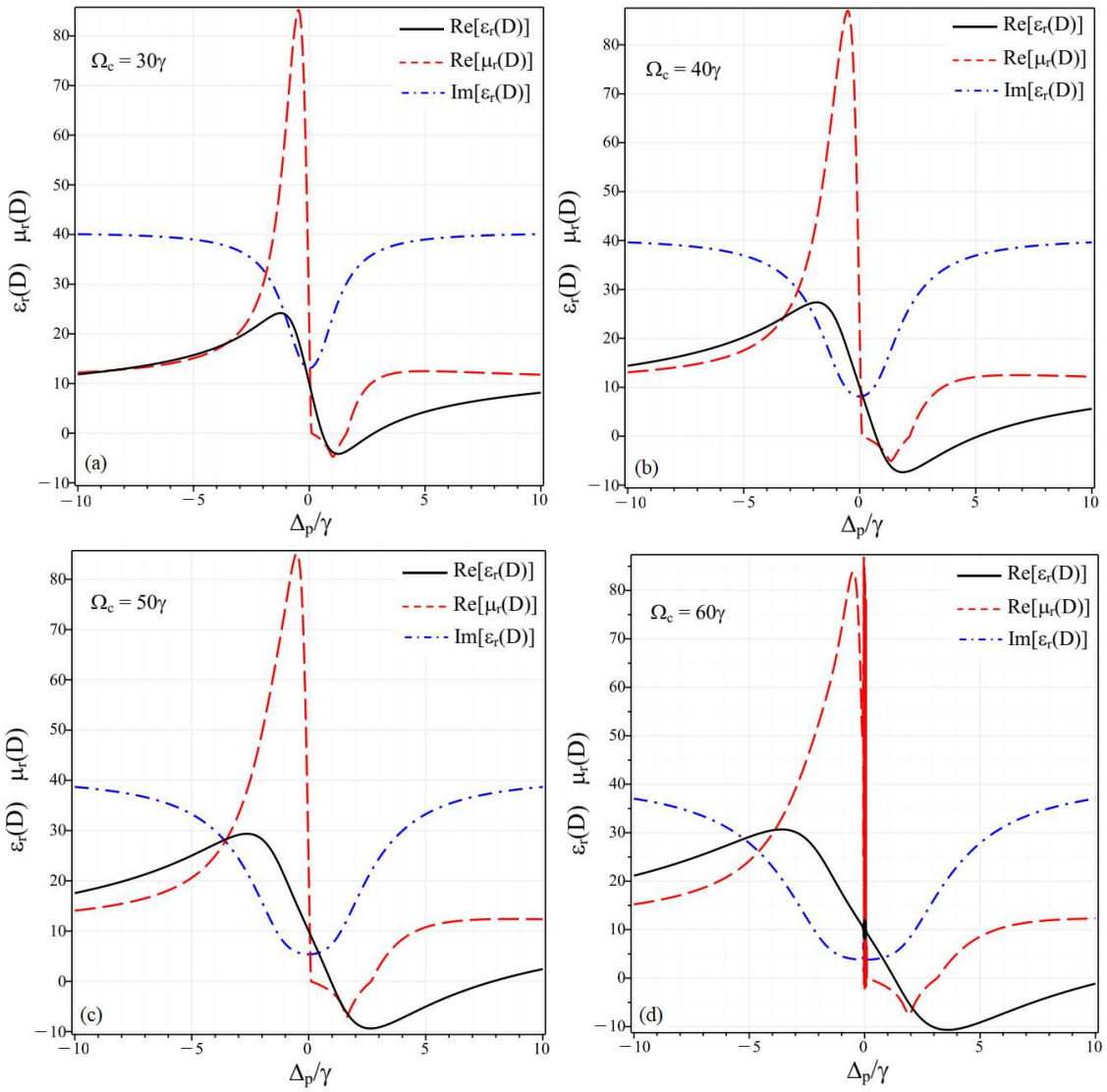

Fig. 2. (Color online) Real parts of the relative permittivity (solid line) and relative permeability (dashed line) as functions of the probe laser detuning, for different values of the coupling field intensity: (a) $\Omega_c = 30\gamma$, (b) $\Omega_c = 40\gamma$, (c) $\Omega_c = 50\gamma$ and (d) $\Omega_c = 60\gamma$. The other parameters used are: $B = 0$ (or $\Delta_B = 0$), $\Delta_c = 0$ and $T = 300\,\mathrm{K}$. The dash-dotted line represents the EIT spectrum.

line) and relative permeability (dashed line) as functions of the probe laser detuning, for various coupling intensities $\Omega_c = 30\gamma$ (a), $\Omega_c = 40\gamma$ (b), $\Omega_c = 50\gamma$ (c) and $\Omega_c = 60\gamma$ (d) at room temperature $T = 300\,\mathrm{K}$. From the solid line $\mathrm{Re}(\varepsilon_r(D))$ and the dashed line $\mathrm{Re}(\mu_r(D))$ in Fig. 2(a) with $\Omega_c = 30\gamma$, it can be observed that both the real parts of the relative permittivity and relative permeability are simultaneously negative in the detuning range $[0.5\gamma, 1.5\gamma]$, indicating that

the medium exhibits a negative refractive index within this spectral region. Similarly, in Fig. 2(b) with $\Omega_c = 40\gamma$, the negative refractive index appears over the range $[0.8\gamma, 2.1\gamma]$. For Fig. 2(c) with $\Omega_c = 50\gamma$, it occurs within $[1\gamma, 2.7\gamma]$, and in Fig. 2(d) with $\Omega_c = 60\gamma$, it extends further to $[1.2\gamma, 4\gamma]$. These results show that as the coupling laser intensity increases, the spectral bandwidth of the negative refractive index also broadens. However, the amplitude of the negative index becomes smaller. This can be explained by the widening of the EIT window (see the dash-dotted lines) with increasing coupling intensity, which leads to a reduced dispersion slope—characterized by the real parts of the relative permittivity and relative permeability.

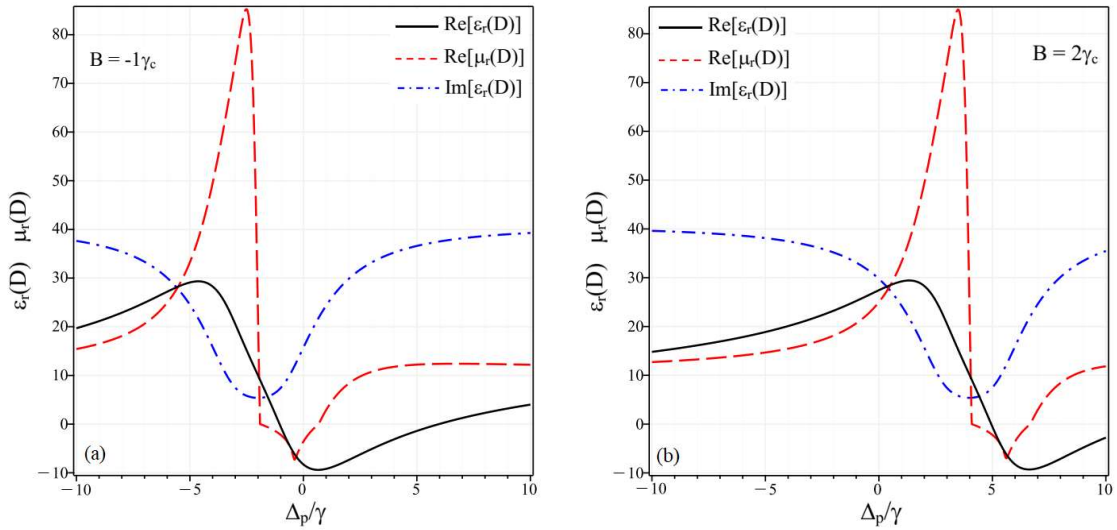

Fig. 3. (Color online) Real parts of the relative permittivity (solid line) and relative permeability (dashed line) as functions of the probe laser detuning for two different values of the magnetic field: (a) $B = -1\gamma_c$ and (b) $B = 2\gamma_c$, while $\Omega_c = 50\gamma$, $\Delta_c = 0$ and $T = 300\,\mathrm{K}$. The dash-dotted line represents the EIT spectrum.

Next, we fix the parameters of the coupling laser at $\Omega_c = 50\gamma$ and $\Delta_c = 0$, and investigate the influence of the external magnetic field on the spectral position of the negative refractive index at room temperature ($T = 300\,\mathrm{K}$). In Fig. 3, we plot the real parts of the relative permittivity (solid line) and relative permeability (dashed line) as functions of the probe laser detuning for two cases: $B = -1\gamma_c$ (a), and $B = 2\gamma_c$ (b). From Fig. 3(a), with $B = -1\gamma_c$, the negative refractive index region shifts to the left along the probe detuning axis, approaching the resonance of the probe field. In contrast, in Fig. 3(b) with $B = 2\gamma_c$, the negative refractive index region shifts to the right, further away from resonance. These results indicate that by adjusting the magnitude and/or the sign of the external magnetic field, the spectral region of negative refractive index can be flexibly shifted to a desired frequency range. Such a shift of the group refractive index regions is associated with the shift of the EIT window position that satisfies the two-photon resonance condition, given by $\Delta_p - \Delta_c - 2\Delta_B = 0$.

In Fig. 4, we analyze the variation of the real parts of the relative permittivity (solid line) and relative permeability (dashed line) as functions of the magnetic field, while keeping the probe

laser detuning fixed at $\Delta_p = \Delta_c = 0$ and the coupling Rabi frequency at $\Omega_c = 50\gamma$, under room temperature condition ($T = 300\,\mathrm{K}$). From Fig. 4, it is evident that both the real parts of the relative permittivity and relative permeability transition from positive to negative and back to positive as the magnetic field changes in both magnitude and sign. In this case, we identify a specific range of magnetic field values where the medium exhibits a negative refractive index, namely in the interval $-1.2\gamma_c < B < -0.2\gamma_c$.

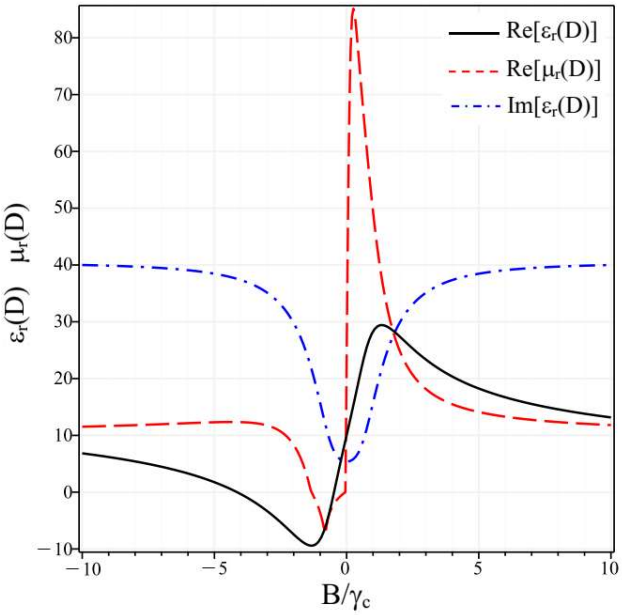

Fig. 4. (Color online) The real parts of the relative permittivity (solid line) and relative permeability (dashed line) as functions of the magnetic field, with other parameters fixed as: $\Omega_c = 50\gamma$, $\Delta_p = \Delta_c = 0$ and $T = 300\,\mathrm{K}$. The dash-dotted line represents the EIT spectrum.

Finally, in Fig. 5, we investigate the influence of temperature on the negative refractive index region of the medium by fixing the laser parameters and plotting the real parts of the relative permittivity and relative permeability at different temperatures, specifically $T = 200\,\mathrm{K}$ (a) and $T = 400\,\mathrm{K}$ (b). At temperature $T = 200\,\mathrm{K}$, the negative refractive index appears in the magnetic field range $[-1.6\gamma_c, -0.2\gamma_c]$, whereas at the higher temperature of $T = 400\,\mathrm{K}$, this range narrows to $[-1.1\gamma_c, -0.5\gamma_c]$. This indicates that as temperature increases, both the bandwidth and the amplitude of the negative refractive index region decrease significantly. This behavior can be explained by the reduction in both the depth and width of the EIT window at higher temperatures (see the dash-dotted line in Fig. 5).

4. Conclusion

In this work, we have investigated the influence of laser intensity, magnetic field, and temperature on the refractive index in a degenerated three-level Λ-type atomic medium. We have

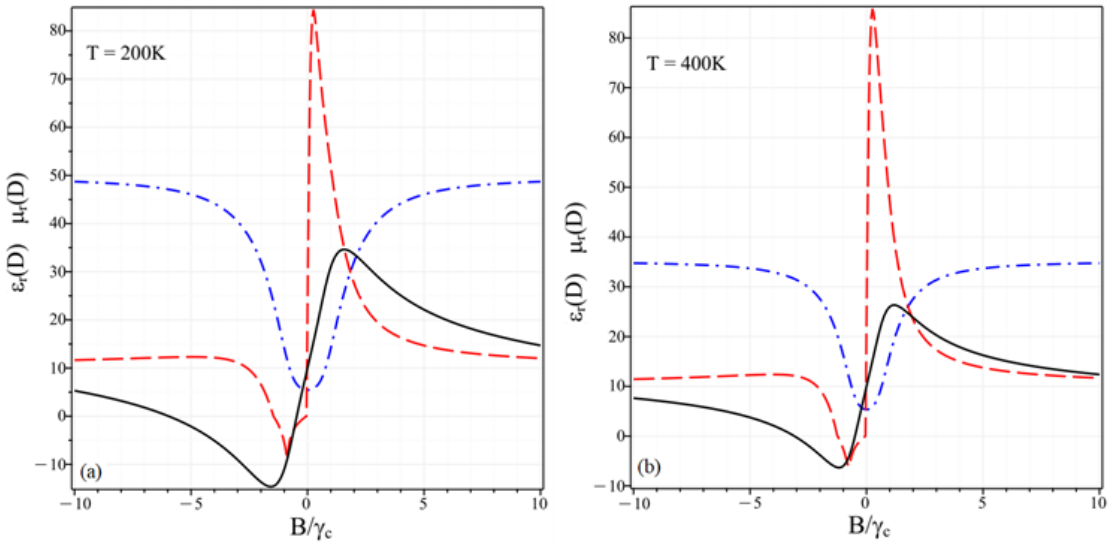

Fig. 5. (Color online) Real parts of the relative permittivity (dotted line) and relative permeability (dashed line) as functions of the magnetic field at two different temperatures: (a) $T = 200\,\mathrm{K}$ and (b) $T = 400\,\mathrm{K}$, while $\Omega_c = 50\gamma$ and $\Delta_p = \Delta_c = 0$. The dash-dotted line represents the EIT spectrum.

identified spectral regions where both the real parts of the relative permittivity and relative permeability are negative, indicating that the medium exhibits a negative refractive index at room temperature. This negative index region can be broadened by increasing the coupling laser intensity, although its amplitude decreases. Moreover, the position of the negative refractive index region can be easily shifted into desired transparent spectral ranges by adjusting the magnitude and/or sign of the external magnetic field. Finally, it is also shown that increasing temperature significantly reduces the spectral range of the negative refractive index.

Acknowledgements

The authors gratefully acknowledge the financial support of the Vingroup Innovation Foundation (VINIF) under project VINIF.2022.DA00076.

Conflict of interest

The authors declare that they have no competing financial interests.

References

[1] J. D. Jackson, *Classical Electrodynamics*. Wiley, New York, 3 ed., 1999.

[2] V. G. Veselago, *The electrodynamics of substances with simultaneously negative values of* ε *and* μ, Sov. Phys. Usp. **10** (1968) 509.

[3] R. A. Shelby, D. R. Smith and S. Schultz, *Experimental verification of a negative index of refraction*, Science **292** (2001) 77.

[4] S. Zhang, W. Fan, N. C. Panoiu, K. J. Malloy, R. M. Osgood and S. R. J. Brueck, *Experimental demonstration of near-infrared negative-index metamaterials*, Phys. Rev. Lett. **95** (2005) 137404.

[5] K. Aydin, I. Bulu and E. Ozbay, *Subwavelength resolution with a negative-index metamaterial superlens*, Appl. Phys. Lett. **90** (2007) 254102.
[6] A. Lakhtakia, *Positive and negative goos-hänchen shifts and negative phase-velocity mediums (alias left-handed materials)*, Int. J. Electron. Commun. (AEU) **58** (2004) 229.
[7] J. B. Pendry, *Negative refraction makes a perfect lens*, Phys. Rev. Lett. **85** (2000) 3966.
[8] Y. P. Yang, J. P. Xu, H. Chen and S. Y. Zhu, *Quantum interference enhancement with left-handed materials*, Phys. Rev. Lett. **100** (2008) 043601.
[9] J. Pendry, *Positively negative*, Nature **423** (2003) 22.
[10] E. Cubukcu, K. Aydin, E. Ozbay, S. Foteinopoulou and C. M. Soukoulis, *Electromagnetic waves: Negative refraction by photonic crystals*, Nature **423** (2003) 604.
[11] G. V. Eleftheriades, A. K. Iyer and P. C. Kremer, *Planar negative refractive index media using periodically l-c loaded transmission lines*, IEEE Trans. Microwave Theory Tech. **50** (2002) 2702.
[12] Z. Li, M. Mutlu and E. Ozbay, *Chiral metamaterials: from optical activity and negative refractive index to asymmetric transmission*, J. Opt. **15** (2013) 023001.
[13] N. H. Bang, D. X. Khoa and L. V. Doai, *Controllable optical properties of multi-electromagnetically induced transparency gaseous atomic medium*, Comm. Phys. **28** (2019) 1.
[14] M. O. Oktel and O. E. Mustecaplioglu, *Electromagnetically induced left-handedness in a dense gas of three-level atoms*, Phys. Rev. A **70** (2004) 053806.
[15] J. Q. Shen, Z. C. Ruan and S. He, *How to realize a negative refractive index material at the atomic level in an optical frequency range*, J. Zhejiang Univ. Science **5** (2004) 1322.
[16] C. M. Krowne and J. Q. Shen, *Dressed-state mixed-parity transitions for realizing negative refractive index*, Phys. Rev. A **79** (2009) 023818.
[17] S. C. Zhao, Z.-D. Liu and Q.-X. Wu, *Zero absorption and a large negative refractive index in a left-handed four-level atomic medium*, J. Phys. B: At. Mol. Opt. Phys. **43** (2010) 045505.
[18] D. X. Khoa, P. V. Trong, L. V. Doai and N. H. Bang, *Electromagnetically induced transparency in a five-level cascade system under doppler broadening: an analytical approach*, Phys. Scr. **91** (2016) 035401.
[19] D. X. Khoa, H. M. Dong, L. V. Doai and N. H. Bang, *Propagation of laser pulse in a three-level cascade inhomogeneously broadened medium under electromagnetically induced transparency conditions*, Optik **131** (2017) 497.
[20] N. T. Anh, L. V. Doai, D. H. Son and N. H. Bang, *Manipulating multi-frequency light in a five-level cascade eit medium under doppler broadening*, Optik **171** (2018) 721.
[21] N. H. Bang, D. X. Khoa, D. H. Son and L. V. Doai, *Effect of doppler broadening on giant self-kerr nonlinearity in a five-level ladder-type system*, Opt. Soc. Am. B **36** (2019) 3151.
[22] N. V. Ai, N. H. Bang and L. V. Doai, *Negative refractive index in a doppler broadened three-level λ-type atomic medium*, Phys. Scr. **97** (2022) 025503.
[23] N. H. Bang and L. V. Doai, *Controlling negative refractive index of degenerated three-level λ-type system by external light and magnetic fields*, Eur. Phys. J. D **75** (2021) 261.
[24] N. H. Bang, N. V. Phu, V. N. Sau, N. T. Cong and L. V. Doai, *Negative refractive index in an inhomogeneously broadened four-level inverted-y atomic medium*, IEEE Photonics Journal **13** (2021) 2200407.
[25] H. G. Al-Toki and A. H. Al-Khursan, *Negative refraction in the double quantum dot system*, Opt. Quant. Electron. **52** (2020) 467.
[26] N. Boutabba, *Controllable refractive index in a four-level left-handed medium using pulse shaping*, J. Opt. **23** (2021) 075504.
[27] U. Hayat, I. Ahmad, H. Ali, R. U. Din and S. Haddadi, *Enhanced negative refraction in one- and two-dimensional chiral atomic lattices*, Results in Physics **56** (2024) 107277.